PROCEDURES FOR ENABLING THE SIMULATION OF MANEUVERS WITH COMPREHENSIVE CODES

C.L. Bottasso, A. Croce, D. Leonello and L. Riviello

Dipartimento di Ingegneria Aerospaziale, Politecnico di Milano, Milano, Italy

Abstract

We describe a computational procedure for the simulation of maneuvers with comprehensive rotorcraft models. Our current approach uses model-based trajectory planning followed by model-based predictive tracking. We describe the predictive tracker and the adaptive reduced model on-line identification procedure. Numerical examples show that rapid and good quality reduced model identification can be achieved by the proposed scheme.

List of Symbols

$\widetilde{(\bullet)}$	system (comprehensive model) quantity
$(\bullet)^{\text{plan}}$	planning problem quantity
$(\bullet)^{\text{track}}$	tracking problem quantity
$(\bullet)^{\text{steer}}$	steering problem quantity
$(\bullet)^{\text{adapt}}$	model adaption problem quantity
$(\bullet)^{*}$	given or desired value
$\widetilde{\boldsymbol{x}}$	system states
$\widetilde{\boldsymbol{\lambda}}$	system Lagrange multipliers
$\widetilde{\boldsymbol{u}}$	system controls
$\widetilde{\boldsymbol{y}}$	system outputs
$\boldsymbol{y}$	reduced model states
$\boldsymbol{u}$	reduced model controls
$\boldsymbol{p}$	reduced model parameters
$\dot{(\bullet)}$	derivative with respect to time
t	time
T_i	initial time
T_f	final time
J	cost function
$(\bullet)_h$	discretized quantity, as obtained by the use of a numerical method

Introduction

We are at present working on a research effort focused on the development of tools for the simulation of maneuvering flight with comprehensive vehicle models [4, 5]. In this paper we describe some recent progress on the problems of trajectory tracking and reduced model identification, which are critical components of our approach to the simulation of maneuvers.

The aero-servo-elastic model $\widetilde{\mathscr{M}}$ of the vehicle is formulated in the framework of flexible multibody system dynamics [1], and it is governed by the following system of differential-algebraic equations:

$$\widetilde{\boldsymbol{f}}(\dot{\widetilde{\boldsymbol{x}}}, \widetilde{\boldsymbol{x}}, \widetilde{\boldsymbol{\lambda}}, \widetilde{\boldsymbol{u}}) = 0, \tag{1a}$$

$$\widetilde{\boldsymbol{c}}(\dot{\widetilde{\boldsymbol{x}}}, \widetilde{\boldsymbol{x}}) = 0, \tag{1b}$$

where the first set of equations, (1a), represents the equations of dynamic equilibrium and the kinematic equations, and the second set, (1b), represents the holonomic and non-holonomic constraint conditions. The servo-structural model of the vehicle is coupled with appropriate aerodynamic models, which in this work are represented by lifting lines and state-based rotor inflow models. The system states are noted $\widetilde{\boldsymbol{x}}$, while $\widetilde{\boldsymbol{\lambda}}$ are the Lagrange multipliers used for enforcing the constraints (1b), and finally the controls are noted $\widetilde{\boldsymbol{u}}$.

Our approach to the simulation of maneuvers is based on the extraction from (1) of a *reduced model* $\mathscr{M}$ that captures the flight mechanics behavior of the vehicle, as described by a set of system outputs $\widetilde{\boldsymbol{y}}$ computed as

$$\widetilde{\boldsymbol{y}} = \widetilde{\boldsymbol{h}}(\widetilde{\boldsymbol{x}}). \tag{2}$$

The reduced model is governed by a set of parametric equations

$$\boldsymbol{f}(\dot{\boldsymbol{y}}, \boldsymbol{y}, \boldsymbol{u}, \boldsymbol{p}) = 0,$$

with states $\boldsymbol{y}$, inputs $\boldsymbol{u}$ and parameters $\boldsymbol{p}$. The free parameters $\boldsymbol{p}$ are computed so as to guarantee the matching of the plant outputs $\widetilde{\boldsymbol{y}}$ and of the reduced model states, i.e. $\widetilde{\boldsymbol{y}} \approx \boldsymbol{y}$, when the two are subjected to the same inputs. We have found that "good" reduced models for rotorcraft applications can be obtained by the use of a reference analytical model augmented with an adaptive neural element, as described below and in References [5, 4].

The reduced model is used for: a) planning of the maneuver path; b) tracking of the planned path. Path planning is formulated as an optimal control problem defined on the reduced vehicle model. Given a current estimate $\boldsymbol{p}^*$ of the reduced model parameters, the planning problem is formulated as follows:

$$\min_{\boldsymbol{u}} J^{\text{plan}}, \tag{3a}$$

$$\text{with: } J^{\text{plan}} = \phi(\boldsymbol{y}, \boldsymbol{u})\big|_T + \int_{T_0}^{T} L(\boldsymbol{y}, \boldsymbol{u})\,\mathrm{d}t, \tag{3b}$$

$$\text{s.t.: } \boldsymbol{f}(\dot{\boldsymbol{y}}, \boldsymbol{y}, \boldsymbol{u}, \boldsymbol{p}^*) = 0, \tag{3c}$$

$$\boldsymbol{g}^{\text{plan}}(\boldsymbol{y}, \boldsymbol{u}, T) \in [\boldsymbol{g}^{\text{plan}}_{\text{min}}, \boldsymbol{g}^{\text{plan}}_{\text{max}}], \tag{3d}$$

$$\boldsymbol{\psi}(\boldsymbol{y}(T_0)) \in [\boldsymbol{\psi}_{0_{\text{min}}}, \boldsymbol{\psi}_{0_{\text{max}}}], \tag{3e}$$

$$\boldsymbol{\psi}(\boldsymbol{y}(T)) \in [\boldsymbol{\psi}_{T_{\text{min}}}, \boldsymbol{\psi}_{T_{\text{max}}}]. \tag{3f}$$

J^{plan} is the planning cost which we seek to optimize, typically a measure of the vehicle performance. The optimization is subjected to the satisfaction of the reduced model vehicle equations of motion (3c), maneuver defining constraints (3d), initial and final conditions (3e) and (3f). The problem is solved numerically using a direct transcription approach [3].

The numerical solution of problem (3) yields a reference trajectory $\boldsymbol{y}_h^*$, that is subsequently tracked by the detailed aero-servo-elastic vehicle model using a model-predictive controller [8], as described below.

As the model $\widetilde{\mathscr{M}}$ is "flown" along $\boldsymbol{y}_h^*$, the reduced model is identified on-line, i.e. the reduced model $\mathscr{M}$ learns the characteristics of $\widetilde{\mathscr{M}}$ through its adaptive nature. Since a new improved estimate of the reduced model is available at the completion of the tracking task, a new planning (3) can be performed, which yields a new tracking trajectory. Iterations between planning and tracking-learning are continued until a desired tolerance in the tracking error is achieved. This iterative procedure results in the Multi-Model Steering Algorithm (MMSA) [4], which can be interpreted as a way to solve the maneuver optimal control problem at the level of the comprehensive vehicle model $\widetilde{\mathscr{M}}$ at acceptable computational costs.

In the following, we describe our current approach to the solution of the tracking problem, and to the associated learning or on-line system identification phase.

Adaptive Tracking with Comprehensive Vehicle Models

Model Predictive Tracking The trajectory tracking problem is formulated within the framework of non-linear model predictive (receding horizon) control. At the current time $t = T_0^{\text{track}}$, the plant states are $\widetilde{\boldsymbol{x}}(T_0^{\text{track}}) = \widetilde{\boldsymbol{x}}_0$, and the corresponding outputs are $\widetilde{\boldsymbol{y}}_0 = \widetilde{\boldsymbol{h}}(\widetilde{\boldsymbol{x}}_0)$. Given the current estimate $\boldsymbol{p}^*$ of the reduced model parameters and the tracking path $\boldsymbol{y}_h^*$ as computed by solving (3), the future control actions are found from the solution of the following discrete model predictive problem on the tracking window $[T_0^{\text{track}}, T^{\text{track}}]$:

$$\min_{\boldsymbol{u}_h} J_h^{\text{track}}, \tag{4a}$$

$$\text{with: } J_h^{\text{track}} = \int_{T_0^{\text{track}}}^{T^{\text{track}}} M(\boldsymbol{y}_h, \boldsymbol{y}_h^*, \boldsymbol{u}_h)\,\mathrm{d}t, \tag{4b}$$

$$\text{s.t.: } \boldsymbol{f}_h(\dot{\boldsymbol{y}}_h, \boldsymbol{y}_h, \boldsymbol{u}_h, \boldsymbol{p}^*) = 0, \tag{4c}$$

$$\boldsymbol{g}_h^{\text{track}}(\boldsymbol{y}_h, \boldsymbol{u}_h) \in [\boldsymbol{g}_{\min}^{\text{track}}, \boldsymbol{g}_{\max}^{\text{track}}], \tag{4d}$$

$$\boldsymbol{y}(T_0^{\text{track}}) = \widetilde{\boldsymbol{y}}_0. \tag{4e}$$

The problem aims at minimizing the tracking cost, J^{track}, which is computed as the integral over the tracking window of the function

$$M(\boldsymbol{y}_h, \boldsymbol{y}_h^*, \boldsymbol{u}_h) = ||\boldsymbol{y}_h - \boldsymbol{y}_h^*||_{S_y^{\text{track}}} + ||\dot{\boldsymbol{u}}_h||_{S_{\dot{u}}^{\text{track}}}.$$

The first term accounts for the tracking error, while the second term penalizes the control rates for ensuring smooth control policies. The solution of this optimization problem satisfies the reduced model governing equations, (4c), together with additional desired input and output constraints, (4d). Notice that the latter effect is difficult to incorporate in other control approaches.

As for the planning problem (3), also problem (4) is solved in this work using a direct transcription method. Since the two problems are similar, the only difference being the cost function and possibly some boundary conditions, they can be solved using the same software.

The numerical solution of (4) yields the optimal control inputs $\boldsymbol{u}_h^*$, which are now used for steering the plant $\widetilde{\mathscr{M}}$ on the short time horizon $[T_0^{\text{steer}}, T^{\text{steer}} < T^{\text{track}}]$. This phase of the problem amounts to the solution of an initial value problem with given control inputs, and it is performed by the coupled aero-servo-elastic multibody-based solver. Once the plant has reached the end of the steering window under the action of the computed control inputs, the model predictive tracking problem (4) is solved again, looking ahead in the future over the tracking horizon shifted forward in time as $T_0^{\text{track}} = T^{\text{steer}}$. This procedure results is a feedback, receding horizon approach, and is graphically depicted in Figure 4.

More precisely, the steering phase involves two steps. The controls $\boldsymbol{u}_h^*$ computed on the grid $\mathscr{T}_h^{\text{track}}$ used for the solution of problem (4) are mapped to the grid $\mathscr{T}_h^{\text{steer}}$ used by the multibody solver, an operation which can be formally written $\boldsymbol{u}_h^*|_{\mathscr{T}_h^{\text{steer}}} = \mathscr{P}(\boldsymbol{u}_h^*|_{\mathscr{T}_h^{\text{track}}})$. The two grids are different, since different time scales need to be resolved in the two cases: while the tracking problem is defined at the level of the reduced model and captures only the flight mechanics scales, the steering problem is defined at the level of the comprehensive model and captures the vibratory response of the aeroelastic vehicle model.

The second step involves the forward-in-time integration of the plant equations starting from the current state $\widetilde{\boldsymbol{x}}_0$, i.e.:

$$\widetilde{\boldsymbol{f}}(\dot{\widetilde{\boldsymbol{x}}}_h, \widetilde{\boldsymbol{x}}_h, \widetilde{\boldsymbol{\lambda}}_h, \boldsymbol{u}_h^*) = 0, \tag{5a}$$

$$\widetilde{\boldsymbol{c}}(\dot{\widetilde{\boldsymbol{x}}}_h, \widetilde{\boldsymbol{x}}_h) = 0, \tag{5b}$$

$$\widetilde{\boldsymbol{x}}(T_0^{\text{steer}}) = \widetilde{\boldsymbol{x}}_0, \tag{5c}$$

which yields a solution in terms of $\widetilde{\boldsymbol{x}}_h$ and $\widetilde{\boldsymbol{\lambda}}_h$. The outputs are readily computed as $\widetilde{\boldsymbol{y}}_h = \widetilde{\boldsymbol{h}}(\widetilde{\boldsymbol{x}}_h)$. The state solution at the end of the steering window, $\widetilde{\boldsymbol{x}}(T^{\text{steer}})$, provides the new initial condition for the next tracking-steering problem. In this work, the numerical integration of the multibody dynamics equations is based on the non-linearly unconditionally stable energy decaying scheme described in [2] and references therein.

<u>Reduced Model</u> The vehicle reduced model is here based on a reference model augmented by a neural network [7]. The governing equations are written

$$\boldsymbol{f}_{\text{ref}}(\dot{\boldsymbol{y}},\boldsymbol{y},\boldsymbol{u}) = \boldsymbol{d}(\boldsymbol{y}^{(n)},\ldots,\boldsymbol{y},\boldsymbol{u}), \tag{6}$$

where $(\cdot)^{(n)}$ indicates the n-th order derivative with respect to time. Notice that higher order derivatives ($n>1$) of the outputs maybe necessary to capture aerodynamic effects, introduced by the coupling of (1) with suitable aerodynamic models. For the rotorcraft applications of this paper, the reference model $\boldsymbol{f}_{\text{ref}}$ is a two-dimensional flight mechanics rigid body model with rotor aerodynamics based on blade element theory with uniform inflow [6]. The reduced model states are defined as the components of the position vector of the vehicle center of gravity, their time rates, the pitch angle, the pitch rate, and the rotor angular velocity. The controls are defined as the main and tail rotor collective, the lateral and longitudinal cyclics and the available power.

In equation (6), the term $\boldsymbol{d}(\boldsymbol{y}^{(n)},\ldots,\boldsymbol{y},\boldsymbol{u})$ represents the reference model defect, i.e. that unknown function that would ensure the matching of reduced states and comprehensive model outputs, $\boldsymbol{y}=\widetilde{\boldsymbol{y}}$. The defect is assumed to be null for the kinematic equations, while it corrects the three dynamic equilibrium equations, namely the horizontal, vertical and pitch equilibrium.

The unknown defect $\boldsymbol{d}$ is approximated using three separate single-hidden-layer neural networks, one for each dynamic equation:

$$d^i(\boldsymbol{y}^{(n)},\ldots,\boldsymbol{y},\boldsymbol{u}) = d^i_{NN}(\boldsymbol{y}^{(n)},\ldots,\boldsymbol{y},\boldsymbol{u}) + \varepsilon^i, \tag{7}$$

where ε^i is the functional reconstruction error for the i-th component. Each single neural network is written as

$$d^i_{NN}(\boldsymbol{y}^{(n)},\ldots,\boldsymbol{y},\boldsymbol{u}) = {\boldsymbol{W}^i}^T \boldsymbol{\sigma}({\boldsymbol{V}^i}^T \boldsymbol{x} + \boldsymbol{a}^i) + \boldsymbol{b}^i,$$
$$i = 1, N_d, \qquad N_d = 3,$$

where $\boldsymbol{W}^i$, $\boldsymbol{V}^i$, $\boldsymbol{a}^i$ and $\boldsymbol{b}^i$ are the matrices of synaptic weights and biases of the i-th network, and $\boldsymbol{\sigma}(\phi) = (\sigma(\phi_1),\ldots,\sigma(\phi_{N_n}))^T$ is the vector-valued function of sigmoid activation functions of the N_n processing elements in the hidden layer. Finally, $\boldsymbol{x} = (\boldsymbol{y}^{(n)T},\ldots,\boldsymbol{y}^T,\boldsymbol{u}^T)^T$ represents the input vector for the networks.

The reduced model governing equations are expressed in a compact form as

$$\boldsymbol{f}(\dot{\boldsymbol{y}},\boldsymbol{y},\boldsymbol{u},\boldsymbol{p}) = 0,$$

where the reduced model parameters $\boldsymbol{p}$ are readily identified with the synaptic weights and biases of the networks:

$$\boldsymbol{p} = (\ldots,{\boldsymbol{p}^i}^T,\ldots)^T,$$
$$\boldsymbol{p}^i = (\ldots,W^i_{jk},V^i_{jk},a^i_{jk},b^i_{jk},\ldots)^T.$$

<u>Model Adaption</u> The fidelity of the reduced model to the plant is crucial for the performance of the model predictive approach, both at the planning and at the tracking levels. In this work, proper matching between the two models is obtained through the adaptive element of the reduced model.

On-line adaption is here obtained based on the minimization of the functional reconstruction error of equation (7), which is accomplished according to the following procedure, illustrated in Figure 5. At first, the multibody outputs $\widetilde{\boldsymbol{y}}^*_h$ obtained during the last steering problem by the time marching solver are processed using a fourth-order Butterworth filter, in order to remove the vibratory response from the flight mechanics solution. Next, the filtered outputs $\mathscr{F}(\widetilde{\boldsymbol{y}}^*_h)$ are projected onto the adaption grid $\mathscr{T}_h^{\text{adapt}}$, which is defined as that portion of the tracking grid that corresponds to the interval $[T_0^{\text{steer}}, T^{\text{steer}}]$. The projection operation can be formally expressed as $\widetilde{\boldsymbol{y}}^*_h|_{\mathscr{T}_h^{\text{adapt}}} = \mathscr{P}^{-1}(\mathscr{F}(\widetilde{\boldsymbol{y}}^*_h|_{\mathscr{T}_h^{\text{steer}}}))$. Time derivatives of $\widetilde{\boldsymbol{y}}^*_h$, as necessary, are now computed based on a suitable interpolation of the filtered and projected solution.

Indicating with T_k^{adapt} the time corresponding to the k-th node of the $\mathscr{T}_h^{\text{adapt}}$ grid, the functional reconstruction error at T_k^{adapt} is now computed as

$$E^i(T_k^{\text{adapt}}) = \left[\varepsilon^i(\widetilde{\boldsymbol{y}}_h^{*(n)},\ldots,\widetilde{\boldsymbol{y}}^*_h,\boldsymbol{u}^*_h)\right]^2\Big|_{T_k^{\text{adapt}}},$$

with

$$\varepsilon^i(T_k^{\text{adapt}}) = \Big[f_{\text{ref}}^i(\widetilde{\boldsymbol{y}}_h^{*(n)},\dots,\widetilde{\boldsymbol{y}}_h^*,\boldsymbol{u}_h^*) - \\ -d_{NN}^i(\widetilde{\boldsymbol{y}}_h^{*(n)},\dots,\widetilde{\boldsymbol{y}}_h^*,\boldsymbol{u}_h^*)\Big]\Big|_{T_k^{\text{adapt}}}.$$

In the previous equations, $\boldsymbol{u}_h^*$ are the inputs computed by solving the model predictive tracking problem (4) and $\widetilde{\boldsymbol{y}}_h^*$ are the corresponding filtered and projected outputs (with their time derivatives) obtained through steering, all quantities being evaluated at time T_k^{adapt}. Notice that, at each step k, the error $E^i(T_k^{\text{adapt}})$ is a sole function of the network parameters $\boldsymbol{p}^i$.

Indicating with $\boldsymbol{p}_k^i$ the currently available estimate of the parameters, an updated estimate is obtained with the steepest-descent correction

$$\boldsymbol{p}_{k+1}^i = \boldsymbol{p}_k^i + \Delta\boldsymbol{p}_k^i,$$

with

$$\Delta\boldsymbol{p}_k^i = -\eta\frac{\partial E^i(T_k^{\text{track}})}{\partial\boldsymbol{p}_k^i},$$

where η is the learning rate.

Numerical Application

We consider a generic medium-size multi-engine utility helicopter in the 9 ton class, with a four bladed articulated rotor. At first, we plan a trajectory using the sole reference model. The maneuver represents a minimum time vertical obstacle avoidance problem. The aircraft starts from and returns to the same level flight trimmed state, as described in [4]. This reference trajectory is now tracked multiple times, to verify the effectiveness of the model adaption procedure.

Tracking and steering windows were selected as $\Delta T^{\text{track}} = 2.0\,\text{sec}$ and $\Delta T^{\text{steer}} = 0.2\,\text{sec}$, respectively. The steering window, which dictates the activation frequency of the predictive controller, is small enough to capture the short period mode of the vehicle. The adaption grid has 2 nodes, and hence 2 successive parameter updates are performed for each steering.

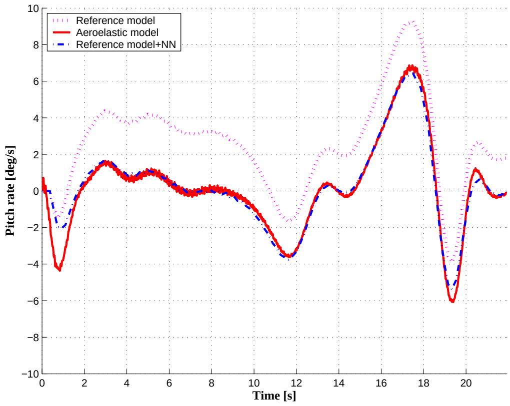

Figure 1: Pitch rate time history for the maneuver tracking problem.

At first we verify the effectiveness of model adaption. Recall that the goal of adaption is to produce a reduced model whose states $\boldsymbol{y}$ match as closely as possible the multibody outputs $\widetilde{\boldsymbol{y}}$, when the two systems are subjected to the same control inputs and starting from the same initial conditions.

The verification of the achievement of good matching performance is demonstrated by Figure 1. The solid line shows the time history of the pitch rate output as obtained by integrating the multibody equations during steering, i.e. by solving equation (5) on each steering window with control inputs $\boldsymbol{u}_h^*$ obtained by the solution of the corresponding model predictive tracking problem (4). The dotted line shows the pitch rate state obtained by the integration on each steering window of the sole reference model, again with the same control inputs $\boldsymbol{u}_h^*$ and starting from the same initial conditions. Finally, the dash-dotted line gives the pitch rate state obtained by integration of the reduced model (reference plus neural defect correction), again from the same initial conditions and with the same control inputs.

Notice that the reference model has reasonably good prediction capabilities. In fact, the dotted line follows quite closely, although not exactly, the solid one: the temporal location of all peaks is excellent, although the curves clearly show a time varying offset. The dif-

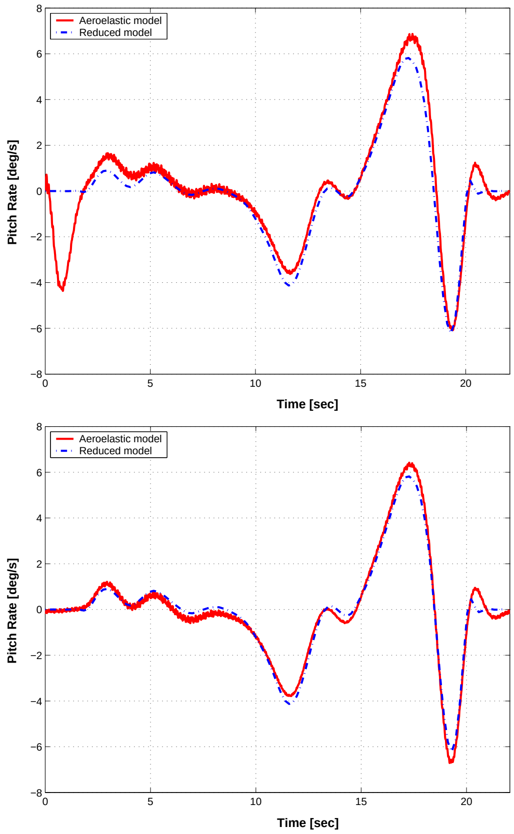

Figure 2: Fuselage pitch rate time history. Top: first maneuver tracking; bottom: fourth maneuver tracking.

ference between the two quantities is due to the approximate nature of the reference model, and must be reduced by the neural element by adaption to capture the reference model defect. By examining the dash-dotted and solid lines one can appreciate how quickly the neural element reduces the gap between the two, and in fact these quantities become extremely similar to each other after the first two seconds of the simulation. The rapidity of the adaption is certainly also due to the reasonably good performance of the reference model, which makes the defect a relatively small quantity, and this in turn makes the adaption a quicker and easier task. From this point of view, we believe that the selection of a good reference model is a key ingredient for the success of the overall reduced model identification and its fast convergence.

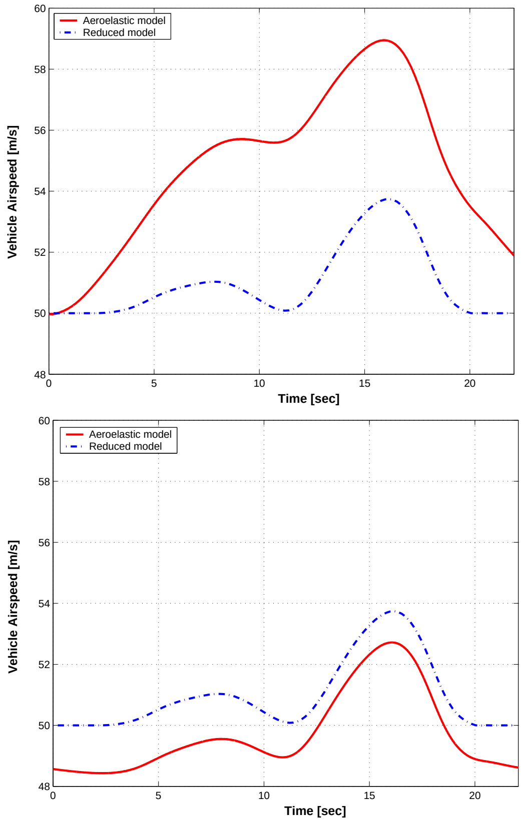

Figure 3: Vehicle airspeed time history. Top: first maneuver tracking; bottom: fourth maneuver tracking.

The quick identification of a good reduced model improves the predictive capabilities of the tracking controller, which in turn reduces the tracking errors. This means that the multibody model can be controlled to better follow the planned path. These effects are demonstrated by Figures 2 and 3, which show the pitch rate and vehicle airspeed time histories, respectively. The to-be-tracked quantities are shown using dash-dotted lines, while the corresponding multibody outputs are plotted using solid lines. Both figures show on top the results for the first tracking, and at bottom the results obtained at the fourth tracking of the same maneuver.

Remember that in this problem the tracking path was generated with the sole reference model solving a performance optimization problem. Since the reference model only roughly approximates the behavior of the multibody model, the planned path can not be exactly tracked by the multibody system, and null tracking errors should not be expected. Therefore, performing multiple trackings of the same path, one should expect to see a reduction of the tracking error up to the point when this error can not be reduced further. In the presence of a "perfect" reduced model, i.e. a model that ensures exact matching of multibody outputs and reduced model states (perfect prediction capabilities), the remaining tracking error is a measure of the infeasibility of the tracking path. This could be reduced only with a new planning, as described in [4].

Examining Figure 2, it appears that the planned pitch rate can be followed very closely even at the first tracking of the whole maneuver (upper figure). An appreciable error is present only in the very first seconds of the simulation, when the neural element has not yet converged.

Figure 3 shows the airspeed tracking. In this case it appears that the initial error in the first seconds of the maneuver, when the neural element has not yet converged, has a less local effect. Observing the figure on the bottom, it is clear that the tracking error has been substantially reduced from the first to the fourth trackings of the maneuver. It was observed that by repeating the maneuver further, this error did not change in an appreciable manner. As previously noted, this remaining tracking error is not due to a deficiency of the reduced model or the tracking controller, but to the effective infeasibility of the planned path for the multibody model.

Conclusions

We have described a procedure for on-line reduced model identification. The reduced model captures the flight mechanics characteristics of a detailed aero-servo-elastic virtual model of a vehicle, and enables its model-based control for the simulation of maneuvering flight conditions.

The reduced model is formulated as a reference model augmented by an adaptive neural element. The use of the reference model ensures that reasonable performance is achieved even before any learning has been possible. Furthermore, it substantially eases the adaption process, since the neural element must only be trained to capture the model defect, which is small if the reference model is adequate.

We have found that the use of independent neural networks for the identification of each single defect component, as opposed to using a multi-output network, speeds up the learning phase at a negligible cost increase. Maximal use of the available information is made by using a cascade steepest-descent update for each coarse grip node in the steering window.

The fast learning convergence and the good observed matching between reduced and full models ensure excellent predictive performance of the controllers, both at the planning level (not investigated in this work), and at the tracking level.

References

[1] Bauchau, O.A., Bottasso, C.L., and Nikishkov, Y.G., "Modeling Rotorcraft Dynamics with Finite Element Multibody Procedures", *Mathematics and Computer Modeling*, Vol. 33, 2001, pp. 1113–1137.

[2] Bauchau, O.A., Bottasso, C.L., and Trainelli, L., "Robust Integration Schemes for Flexible Multibody Systems", *Computer Methods in Applied Mechanics and Engineering* Vol. 192, 2003, pp. 395–420.

[3] Betts, J.T., *Practical Methods for Optimal Control Using Non-Linear Programming*, SIAM, Philadelphia, PA, 2001.

[4] Bottasso, C.L., Chang, C.-S., Croce, A., Leonello, D., and Riviello, L., "Adaptive

Planning and Tracking of Trajectories for the Simulation of Maneuvers with Multibody Models", *Computer Methods in Applied Mechanics and Engineering*, accepted, to appear in the special issue "Computational Multibody Dynamics".

[5] Bottasso, C.L., and Croce, A., "Two-Level Model-Based Control of Flexible Multibody Systems", 6th European Conference on Structural Dynamics (EURODYN 2005), Paris, France, September 4–7, 2005.

[6] Bottasso, C.L., Croce, A., Leonello, D., and Riviello, L., "Optimization of Critical Trajectories for Rotorcraft Vehicles", *Journal of the American Helicopter Society*, Vol. 50, 2005, pp. 165–177.

[7] Fausett, L., *Fundamentals of Neural Networks*, Prentice Hall, New York, NY, 1994.

[8] Findeisen, R., Imland, L., Allgöwer, F., and Foss, B.A., "State and Output Feedback Nonlinear Model Predictive Control: An Overview", *European Journal of Control*, Vol. 9, 2003, pp. 190–207.

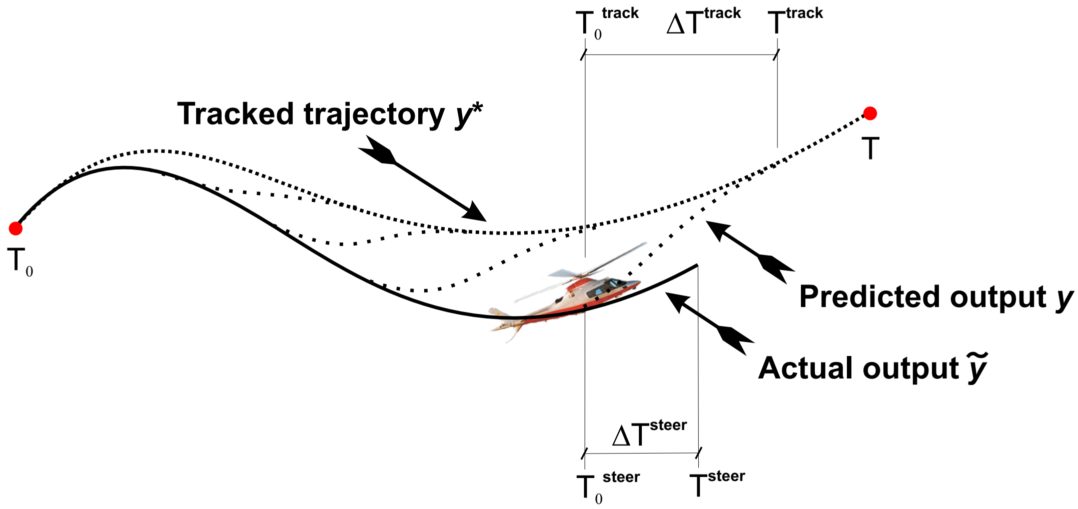

Figure 4: Schematic illustration of model predictive tracking, with the indication of the to-be-tracked (planned) trajectory and the system (actual) and reduced model (predicted) output time histories.

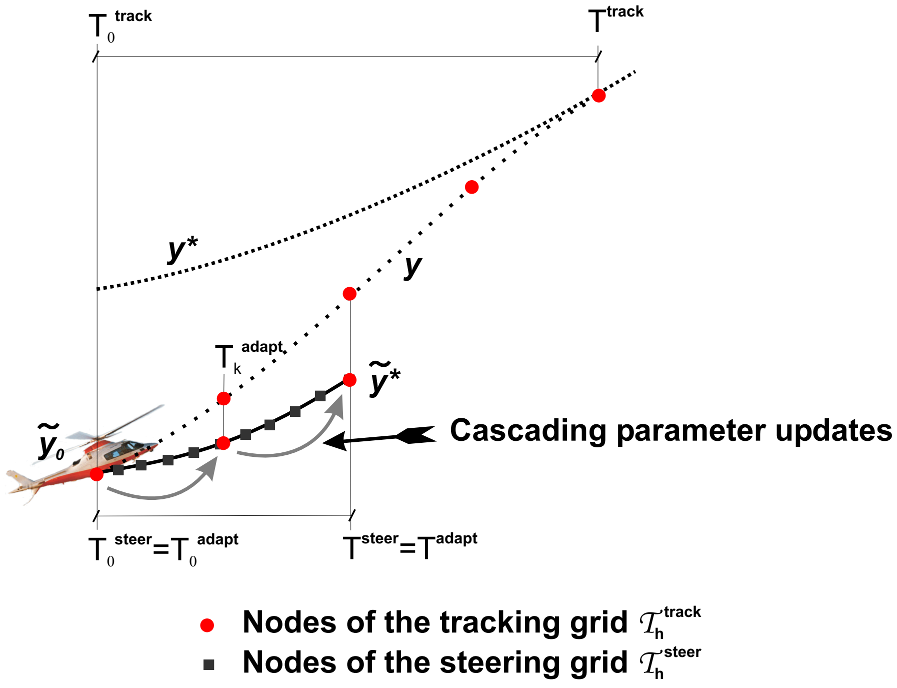

Figure 5: Illustration of model adaption during tracking, showing the details of the different temporal grids.